

Article

Biologically-Inspired Intelligent Flocking Control for Networked Multi-UAS with Uncertain Network Imperfections

Mohammad Jafari ^{1,*}  and Hao Xu ²

¹ Department of Applied Mathematics, Jack Baskin School of Engineering, University of California, Santa Cruz, CA 95064, USA

² Department of Electrical and Biomedical Engineering, University of Nevada, Reno, NV 89557, USA; haoxu@unr.edu

* Correspondence: mjafari1@ucsc.edu

Received: 26 July 2018; Accepted: 27 September 2018; Published: 29 September 2018



Abstract: In this paper, a biologically-inspired distributed intelligent control methodology is proposed to overcome the challenges, i.e., networked imperfections and uncertainty from the environment and system, in networked multi-Unmanned Aircraft Systems (UAS) flocking. The proposed method is adopted based on the emotional learning phenomenon in the mammalian limbic system, considering the limited computational ability in the practical onboard controller. The learning capability and low computational complexity of the proposed technique make it a propitious tool for implementing in real-time networked multi-UAS flocking considering the network imperfection and uncertainty from environment and system. Computer-aid numerical results of the implementation of the proposed methodology demonstrate the effectiveness of this algorithm for distributed intelligent flocking control of networked multi-UAS.

Keywords: networked multi-unmanned aircraft systems; flocking control; intelligent control; biologically-inspired reinforcement learning

1. Introduction

1.1. Motivation

Distributed coordination of networked multi-Unmanned Aircraft Systems (UAS) has been studied by diverse research communities in recent years [1–4]. Due to the broad applications of *flocking* in real-world scenarios, most of the networked multi-UAS control methodologies are adopted based on the mathematical model of flocking [5–7]. In general, three basic rules (i.e., *separation*, *alignment*, and *cohesion*) are considered for simulating the flocking behavior [1] which are observed in many living beings (i.e., birds, fish, bacteria, and insects) [8].

Several research groups have been contributed for improving the flocking behavior of networked multi-UAS in recent years [9–12]. Groups of aircrafts, in many applications involving networked multi-UAS, require communicating in order to successfully accomplish their assigned tasks. Network imperfection, e.g., delay, commonly exists in communication due to the limited communication resource and heavy traffic in the network [13,14]. As a result, it is of paramount importance to address the challenges of network-induced delay and taking the influence of network-induced delays into account in designing control algorithms for multi-unmanned aircraft systems. Besides network imperfections, the uncertainty from the complex environment and system dynamics is another critical challenge and cannot be ignored in advanced applicable control development. Therefore, it is important to consider the uncertainties from the environment and system in designing control algorithms.

1.2. Related Works

Diverse research groups have attempted to address the issues arising from the effects of network-induced delay in flocking control of multi-unmanned aircraft systems/multi-agent systems. For example, delay-independent flocking control of multi-agent systems have been addressed in [15,16]. Closely related, a distributed control design for the discrete-time directed multi-agent systems with distributed network-induced delay has been proposed in [17]. The authors in [18] presented a distributed algorithm for the sensor networks by considering the effects of the imperfect communication such as link failures and channel noise. In [19], the authors studied the design of distributed formation recovery control for nonlinear heterogeneous multi-agent systems. A distance constrained based adaptive flocking control for the multi-agent system with network-induced delay was investigated in [20]. Recently, coordinated control of two-wheel mobile robots with input network-induced delay was presented in [21]. Although all of these proposed methods perform well dealing with the effects of network-induced delay, they still need the detailed information of the system. In this regard, the development of control strategies for dealing with the network-induced delay with less dependency on the full knowledge of the system dynamics is of paramount importance.

In recent years, intelligent approaches have been extensively utilized for successfully solving diverse complex problems [22–24]. Among them, biologically-inspired intelligent approaches have received tremendous interest by many researchers because of their inherent potential to deal with computationally complex systems. *Emotional Learning* is one such approach, which takes advantage of a computational model of the amygdala in the mammalian limbic system [25]. This model, known as Brain Emotional Learning Based Intelligent Controller (BELBIC), consists of the *Amygdala*, *Orbitofrontal Cortex*, *Thalamus*, and *Sensory Input Cortex* as its main components. From a control systems point of view, BELBIC is a model-free controller (i.e., model dynamics are fully or partially unknown) that has shown promising performance under noise and system uncertainty [26].

Sensory Inputs (SI) and *Emotional Signal (ES)* are two main inputs to the BELBIC model, and it is shown that the multi-objective problems could be solved by defining appropriate *SI* and *ES* [27,28]. The flexibility in assigning different *SI* and *ES* makes this controller a practical tool for implementation in real-time applications. Furthermore, BELBIC could effectively control a system even when the states of the system and the controller performance feedback are the only available information [26]. In addition, compared to other existing learning-based intelligent control methods, the computational complexity of BELBIC is on the order of $O(n)$, which makes it a suitable approach for real-time implementation.

1.3. Main Contributions

The main contribution of this paper is to develop a model-free distributed intelligent control methodology to overcome the challenges including the network-induced delay and uncertainties from the environment and system in networked multi-UAS. To this end, we propose a biologically-inspired distributed intelligent controller, which takes advantage of the computational model of emotional learning in the mammalian limbic system. Our recent work in [29] introduced the theoretical framework for the flocking control for networked multi-UAS using BELBIC. These results are improved upon and extended in this paper for accomplishing an intelligent and practical flocking of networked multi-UAS, when subjected to impacts from uncertain network imperfections. The proposed methodology has a low computational complexity, which makes it a promising method for real-time applications. Furthermore, keeping the system complexity in a practically achievable limit, the proposed method delivers a controller with multi-objective properties (i.e., control effort optimization, network-induced delay handling, and noise/disturbance rejection). Moreover, we provided the Lyapunov stability analysis to demonstrate that our proposed methodology guarantees the convergence of the designed control signals as well as maintaining the system stability during the learning. The learning capability of the proposed approach is validated for flocking control of multi-unmanned aircraft systems influenced by the network-induced delay with promising performance. Computer-based numerical results of

the implementation of the proposed methodology demonstrate the effectiveness of this algorithm for distributed intelligent flocking control of networked multi-UAS.

In other words, the solution proposed in this paper is a model-free distributed intelligent controller, which provides the following benefits:

- The knowledge of system dynamics is not fully or partially required.
- It has the capabilities of overcoming the network-induced delay, handling the uncertainties, and noise/disturbance rejection.
- It is appropriate for real-time implementation due to its low computational complexity (i.e., the developed algorithm is a real-time applicable learning technique).
- It ensures the stability of the system.

The rest of the paper is organized as follows. Section 2 presents the problem formulation and some preliminaries about flock modeling with network-induced delay and emotional learning. Our main contribution is introduced in Section 3, which consists of a distributed intelligent flocking control strategy based on emotional learning. Section 4 presents numerical simulation results. The conclusions of the paper and future directions of our work are provided in Section 5.

2. Problem Formulation and Preliminaries

In this section, some preliminaries are provided and the problem formulation is briefly discussed. First, the dynamic of the networked multi-UAS is given; then, flock topology is modeled by means of a dynamic graph. Next, network-induced delay and BELBIC model are introduced, and, ultimately, the problem is formulated.

2.1. Flock Modelling

Assuming the movement of the flock in an m -dimensional space ($m = 2, 3$), the equation of motion of the i th agent with continuous-time double integrator dynamics could be described according to the following set of equations:

$$\begin{cases} \dot{q}_i(t) = p_i(t), \\ \dot{p}_i(t) = u_i(t) \end{cases}, i = 1, 2, \dots, n, \quad (1)$$

where $u_i(t) \in \mathbb{R}^m$ is the control input, $\{q_i(t), p_i(t)\} \in \mathbb{R}^m$ are position, and velocity of the i th agent, respectively. Consider a dynamic graph $\mathcal{G}(v, \varepsilon(t))$ that consists of a set of vertices $v = \{1, 2, \dots, n\}$, and edges $\varepsilon(t) \subseteq \{(i, j) : i, j \in v, j \neq i\}$. Each vertex represents an agent of the flock while a communication link between a pair of agents is represented by an edge.

$N_i^\alpha(t) = \{j \in v_\alpha : \|q_j(t) - q_i(t)\| < r, j \neq i\}$ is the neighborhood set of agent i , where the range of interaction between agents i and agent j is defined by a positive constant r , and $\|\cdot\|$ is the Euclidean norm in \mathbb{R}^m . Solving the set of algebraic conditions: $\|q_j(t) - q_i(t)\| = d \quad \forall j \in N_i^\alpha(t)$, we could describe the geometric model of the flock, i.e., the α -lattice [3], where the distance between two neighbors i and j is represented by a positive constant d .

To avoid the singularity of the collective potential function at $q_i(t) = q_j(t)$, the σ -norm (i.e., $\|\cdot\|_\sigma$) is defined where $\|z\|_\sigma = \frac{1}{\epsilon}[\sqrt{1 + \epsilon\|z\|^2} - 1]$, and ϵ is a positive constant. To resolve the singularity problem, the set of algebraic conditions can be rewritten as: $\|q_j(t) - q_i(t)\|_\sigma = d_\alpha \quad \forall j \in N_i^\alpha(t)$.

A smooth collective potential function $V(q) = \frac{1}{2} \sum_i \sum_{j \neq i} \psi_\alpha(\|q_j(t) - q_i(t)\|_\sigma)$ can be obtained by considering the above-mentioned constraints, where $\psi_\alpha(z) = \int_{d_\alpha}^z \phi_\alpha(s) ds$ is a smooth pairwise potential function with $\phi_\alpha(z) = \rho_h(z/r_\alpha)\phi(z - d_\alpha)$, $\phi(z) = \frac{1}{2}[(a+b)\sigma_1(z+c) + (a-b)]$, and $\sigma_1(z) = z/\sqrt{1+z^2}$.

A possible choice for defining $\rho(z)$, which is a scalar bump function that smoothly varies between $[0,1]$, is [3]:

$$\begin{cases} 1, & z \in [0, h), \\ \frac{1}{2} \left[1 + \cos \left(\pi \frac{(z-h)}{(1-h)} \right) \right], & z \in [h, 1], \\ 0, & \text{otherwise.} \end{cases} \quad (2)$$

$u_i(t) = u_i^\alpha + u_i^\beta + u_i^\gamma$ is the flocking control algorithm introduced in [3], which consists of three main terms:

- (i). u_i^α is the interaction component between two α -agents and is defined as follows:

$$\begin{aligned} u_i^\alpha &= c_1^\alpha \sum_{j \in N_i^\alpha} \phi_\alpha(\|q_j(t) - q_i(t)\|_\sigma) \mathbf{n}_{i,j} \\ &+ c_2^\alpha \sum_{j \in N_i^\alpha} a_{ij}(q)(p_j(t) - p_i(t)), \end{aligned} \quad (3)$$

where c_1^α and c_2^α are positive constants. The terms $\mathbf{n}_{i,j}$ and $a_{ij}(q)$ are vector and the elements of the spatial adjacency matrix $A(q)$, respectively, which are described as follows:

$$\begin{aligned} \mathbf{n}_{i,j} &= \frac{q_j(t) - q_i(t)}{\sqrt{1 + \epsilon \|q_j(t) - q_i(t)\|^2}}, \\ a_{ij}(q) &= \rho_h(\|q_j(t) - q_i(t)\|_\sigma / r_\alpha) \in [0, 1], j \neq i, \end{aligned}$$

where $r_\alpha = \|r\|_\sigma$, and $a_{ii}(q) = 0$ for all i and q .

- (ii). u_i^β is the interaction component between the α -agent and an obstacle (named the β -agent) and is defined as follows:

$$\begin{aligned} u_i^\beta &= c_1^\beta \sum_{k \in N_i^\beta} \phi_\beta(\|\hat{q}_{i,k} - q_i\|_\sigma) \hat{\mathbf{n}}_{i,k} \\ &+ c_2^\beta \sum_{k \in N_i^\beta} b_{i,k}(q)(\hat{p}_{i,k} - p_i), \end{aligned} \quad (4)$$

where c_1^β and c_2^β are positive constants. $\hat{q}_{i,k}$ and $\hat{p}_{i,k}$ are position, and velocity of the k th obstacle (i.e., β -agent), respectively. The terms $\hat{\mathbf{n}}_{i,k}$ and $b_{i,k}(q)$ are vector and the elements of the heterogeneous adjacency matrix $B(q)$, respectively, which are defined as follows:

$$\begin{aligned} \hat{\mathbf{n}}_{i,k} &= \frac{\hat{q}_{i,k} - q_i}{\sqrt{1 + \epsilon \|\hat{q}_{i,k} - q_i\|^2}}, \\ b_{i,k}(q) &= \rho_h(\|\hat{q}_{i,k} - q_i\|_\sigma / d_\beta). \end{aligned}$$

$\phi_\beta(z) = \rho_h(z/d_\beta)(\sigma_1(z - d_\beta) - 1)$ is a repulsive action function and $N_i^\beta = \{k \in v_\beta : \|\hat{q}_{i,k} - q_i\| < r'\}$ is the set of β -neighbors of an α -agent i , where the range of interaction of an α -agent with obstacles is the positive constant r' . Here, $d_\beta = \|d'\|_\sigma$, and $r_\beta = \|r'\|_\sigma$

- (iii). u_i^γ is a goal component that consists of a distributed navigational feedback term and is defined as follows:

$$u_i^\gamma = -c_1^\gamma \sigma_1(q_i - q_r) - c_2^\gamma (p_i - p_r), \quad (5)$$

where c_1^γ and c_2^γ are positive constants.

More detailed studies about flocking control algorithms can be found in [3].

Remark 1. In practical networked multi-UAS flocking control systems, due to the complexity of the overall system, autonomous agents are commonly described by the double integrator dynamics. Since our analysis is focused on developing an intelligent distributed controller for flocking of networked multi-UAS, in this paper, the double integrator dynamics is adopted. Considering the fact that the double integrator dynamics is a very reduced dynamics of the quad rotorcrafts, one can extend our results by employing model-free inner-loop controllers in [23,30], etc.

2.2. Network-Induced Delays

Assuming that the state of agent i gets to agent j after passing through a communication channel with network-induced delay $\tau_{ij} > 0$, the u_i^α could be rewritten as:

$$u_i^\alpha = c_1^\alpha \sum_{j \in N_i^\alpha} \phi_\alpha(\|q_j(t - \tau_{ij}) - q_i(t - \tau_{ij})\|_\sigma) \mathbf{n}_{i,j} + c_2^\alpha \sum_{j \in N_i^\alpha} a_{ij}(q)(p_j(t - \tau_{ij}) - p_i(t - \tau_{ij})). \tag{6}$$

In this paper, we consider the case where the network-induced delays in all channels are equal to $\tau > 0$. Although the delay is deterministic, it is unknown. The proposed method can effectively handle this unknown delay.

2.3. Brain Emotional Learning-Based Intelligent Controller

Brain Emotional Learning Based Intelligent Controller (BELBIC) is one of the neurobiologically-motivated intelligent methodologies, which is based on the computational model of emotional learning observed in the mammalian limbic system proposed in [25]. This model (depicted in Figure 1), has two main parts: *Amygdala*, and *Orbitofrontal Cortex*. *Amygdala* is responsible for immediate learning, while *Orbitofrontal Cortex* is responsible for inhibition of any inappropriate learning happening in the *Amygdala*. *Sensory Inputs (SI)* and *Emotional Signal (ES)* are two main inputs to the BELBIC model.

The output of the BELBIC model (MO) can be defined as

$$MO = \sum_l A_l - \sum_l OC_l, \tag{7}$$

which is calculated by the difference between the *Amygdala* outputs (A_l) and the *Orbitofrontal Cortex* outputs (OC_l). Here, l is the number of sensory inputs.

The *Orbitofrontal Cortex* and the *Amygdala* outputs are calculated by the summation of all their corresponding nodes, where the output of each node is described as:

$$A_l = V_l SI_l, \tag{8}$$

$$OC_l = W_l SI_l, \tag{9}$$

where SI_l is the l th sensory input, V_l is the weight of the *Amygdala*, and W_l is the weight of the *Orbitofrontal Cortex*. The following equations are employed for updating V_l and W_l , respectively:

$$\Delta V_l = K_v SI_l \max\left(0, ES - \sum_l A_l\right), \tag{10}$$

$$\Delta W_l = K_w SI_l (MO - ES), \tag{11}$$

where K_w and K_v are the learning rates.

The maximum of all SI_i is another input considered in the model. This signal (i.e., A_{th}), which is directly sent from the Thalamus to the Amygdala, is defined as:

$$A_{th} = V_{th} \max(SI_i), \tag{12}$$

where V_{th} is the weight and the corresponding update law is the same as Equation (10).

Several techniques have been adopted for tuning the BELBIC parameters [26,31–35]. In this paper, to significantly reduce the computational complexity, a heuristic approach is utilized for tuning the BELBIC parameters.

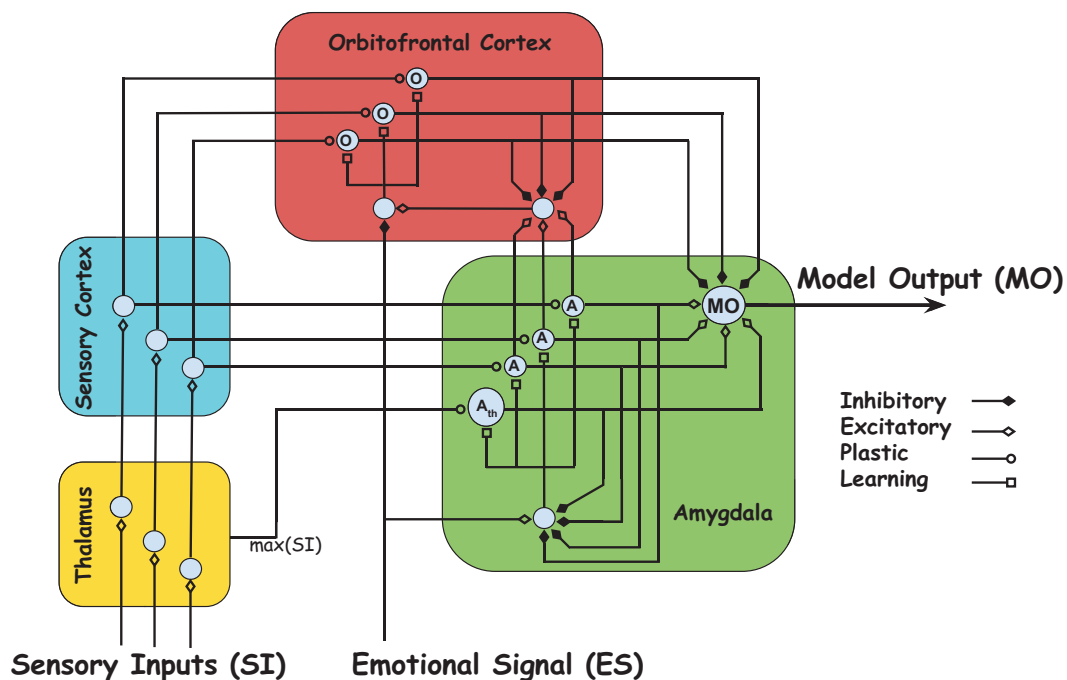


Figure 1. Computational model of emotional learning.

2.4. Objectives

The objective is to design a biologically-inspired distributed intelligent controller for flocking control of multi-unmanned aircraft systems (i.e., $u_i, i = 1, \dots, n$ and n is the number of UASs), specifically, in the events of network-induced delay. The proposed intelligent control method is leveraging the computational model of emotional learning in the mammalian limbic system (i.e., BELBIC) introduced in Section 2.3, and is applied to the flocking model of networked multi-UAS described in Section 2.1.

In other words, the solution proposed in this paper is a model-free distributed intelligent controller, which is designed to maintain the motion of all agents in the flock in the events of network-induced delay.

3. Distributed Intelligent Flocking Control of Networked Multi-UAS Using Emotional Learning

3.1. System Design

Specifically, our focus is on the design of a biologically-inspired distributed intelligent controller for flocking of networked multi-UAS by using BELBIC because the implementation of it could be accomplished without increasing the complexity of the overall system. The BELBIC architecture implemented in this work is shown in Figure 2. This figure demonstrates a closed loop configuration that consists of the following blocks: (i) BELBIC block, (ii) Sensory inputs (SI) function block,

(iii) Emotional signal (ES) generator block, and finally (iv) a block for the plant. This architecture implicitly demonstrates the overall emotional learning based control concept, which consists of the action selection mechanism, the critic, and the learning algorithm [26].

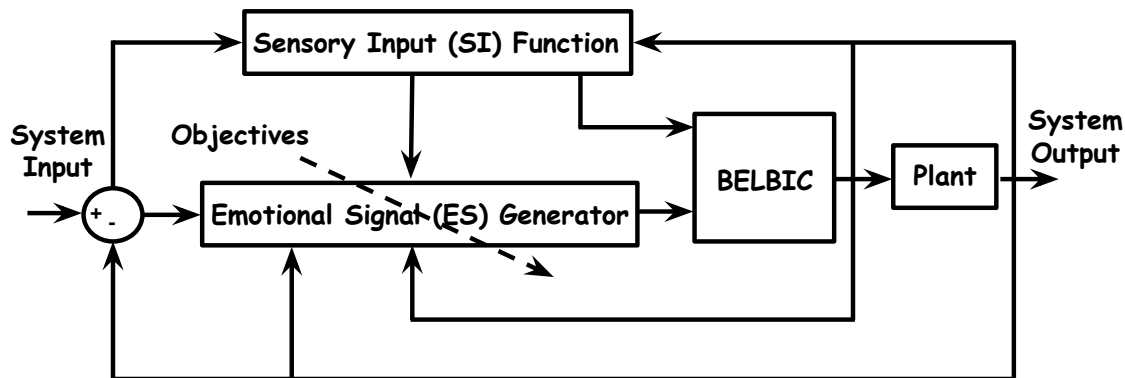


Figure 2. Brain Emotional Learning Based Intelligent Controller (BELBIC) in the control loop.

3.2. Emotional Signal and Sensory Input Development

Fundamentally, BELBIC is an action selection technique, in which action is produced based on the sensory input (SI) and the emotional signal (ES). The general forms of SI and ES are given as follows:

$$SI = G(e, r, y, u), \tag{13}$$

$$ES = F(e, r, y, u), \tag{14}$$

where e is the system error, r is the system input, y is the system output, and u is the control effort.

The control objectives (e.g., reference tracking and optimal control) could implicitly be decided by choosing the adequate ES. For example, it is possible to choose the ES for achieving a better reference tracking performance, for reducing the overshoot, and/or for the energy expense minimization, among others.

Aiming at designing a model-free distributed intelligent control for flocking control of multi-unmanned aircraft systems, the proposed biologically-inspired technique will focus on improving: (i) reference tracking performance, (ii) network-induced delay handling, and (iii) disturbance rejection.

To accomplish these objectives, for each of the control inputs (i.e., $\{u_1, \dots, u_n\}$), the SI_i and ES_i , will be designed as:

$$SI_i = K_{SI}^\alpha u_i^\alpha + K_{SI}^\beta u_i^\beta + K_{SI}^\gamma u_i^\gamma, \tag{15}$$

$$ES_i = K_{ES}^\alpha u_i^\alpha + K_{ES}^\beta u_i^\beta + K_{ES}^\gamma u_i^\gamma, \tag{16}$$

where $i = \{1, \dots, n\}$, K_{SI}^α , K_{SI}^β , K_{SI}^γ , K_{ES}^α , K_{ES}^β , and K_{ES}^γ are positive gains. The ES will change its impact on the system behavior by assigning different values to these positive gains. In this work, different gains are assigned for each one of the control inputs (i.e., u_i , $i = 1, \dots, n$) of the system.

It should be mentioned that we designed the ES in such a way that the increase in reference tracking error will generate a *negative emotion* in the system, which is then taken as evidence for the unsatisfactory performance of the system. Therefore, the proposed controller will behave in such a way that it will always minimize the negative emotion, which leads to the satisfactory performance of the system.

3.3. Learning-Based Intelligent Flocking Control

In flocking control of networked multi-UAS, multiple performance considerations have to be taken into account all at the same time; therefore, it is a very interesting case for using biologically-inspired learning-based multi-objective methodologies like BELBIC. Designing a model-free distributed intelligent control for flocking of networked multi-UAS by considering the network-induced delay, in addition to designing a suitable controller for real-time implementation, encourages us to take advantage of the computational model of emotional learning in the mammals' limbic system, i.e., BELBIC.

From Equations (15) and (16), the BELBIC-inspired distributed intelligent flocking control strategy for networked multi-UAS is defined as

$$\begin{aligned} u_i^{BEL} &= \sum_i V_i \cdot SI_i - \sum_i W_i \cdot SI_i \\ &= \sum_i V_i \cdot \left(K_{SI}^\alpha \cdot u_i^\alpha + K_{SI}^\beta \cdot u_i^\beta + K_{SI}^\gamma \cdot u_i^\gamma \right) \\ &\quad - \sum_i W_i \cdot \left(K_{SI}^\alpha \cdot u_i^\alpha + K_{SI}^\beta \cdot u_i^\beta + K_{SI}^\gamma \cdot u_i^\gamma \right). \end{aligned} \quad (17)$$

Here, $i = 1, \dots, n$ makes reference to each control input and n is the number of UASs. Considering the results obtained in Theorem 1 and by substituting the Emotional Signal with Equation (16), the BELBIC model output of the distributed intelligent control for flocking of networked multi-UAS could be obtained as follows:

$$MO = ES_i = K_{ES}^\alpha u_i^\alpha + K_{ES}^\beta u_i^\beta + K_{ES}^\gamma u_i^\gamma, \quad (18)$$

which clearly satisfies our goal of distributed intelligent flocking control. In other words, the model output accomplished all the flocking properties i.e., Collision Avoidance, Obstacle Avoidance, and Navigational Feedback.

The overall model-free biologically-inspired distributed intelligent flocking control methodology proposed in this paper is summarized as a pseudo-code in Algorithm 1.

Algorithm 1 : The BELBIC-inspired methodology for distributed intelligent flocking control of networked multi-UAS.

Initialization:

Set $W_i = 0$, $V_{th} = 0$, and $V_i = 0$, for $i = 1, \dots, n$.

Define τ = network-induced delay.

Define ES_i = Objective function, for $i = 1, \dots, n$.

for each iteration $t = t_s$ **do**

for each agent i **do**

 Compute $SI_i = K_{SI}^\alpha u_i^\alpha + K_{SI}^\beta u_i^\beta + K_{SI}^\gamma u_i^\gamma$

 Compute $ES_i = K_{ES}^\alpha u_i^\alpha + K_{ES}^\beta u_i^\beta + K_{ES}^\gamma u_i^\gamma$

 Compute $A_i = V_i SI_i$

 Compute $A_{th} = V_{th} \max(SI_i)$

 Compute $OC_i = W_i SI_i$

 Compute $BEL_i = \sum_i A_i - \sum_i OC_i$

 Update V_i

 Update V_{th}

 Update W_i

end for

end for

3.4. Stability Analysis

Theorem 1 is presenting the convergence of the weights of the Amygdala (V_l) and the Orbitofrontal Cortex (W_l). Theorem 2 is providing the closed-loop stability of the proposed controller and Remark 2 explains how the proposed method converges to distributed intelligent flocking control of networked multi-UAS.

Theorem 1. *Given the BELBIC design as Equations (15)–(18), there exists the positive BELBIC tuning parameters, K_v, K_w satisfying*

$$\begin{aligned} \text{I.} \quad & \left| \left[1 - K_v (S I_l)^2 \right] \right| < 1, \\ \text{II.} \quad & \left| \left[1 - K_w (S I_l)^2 \right] \right| < 1, \end{aligned}$$

such that the BELBIC estimated weights of the Amygdala (V_l) and the Orbitofrontal Cortex (W_l) converge to the desired targets asymptotically.

Proof. See Appendix A. \square

Theorem 2. *(Closed-loop Stability): Given that the initial networked multi-UAS state $x(0)$ and the BELBIC estimated weights of the Amygdala ($V_l(0)$) and the Orbitofrontal Cortex ($W_l(0)$) are bounded in the set Λ , let the BELBIC be tuned and estimated control policy be given as Equations (10), (11) and (17), respectively. Then, there exist positive constants, K_v, K_w , satisfying Theorem 1 such that networked multi-UAS state, $x(t)$ and BELBIC weight estimation errors are all asymptotically stable.*

Proof. See Appendix B. \square

Remark 2. *Based on the BELBIC theory [26] and (Equation (17)), the distributed intelligent flocking control of networked multi-UAS can be obtained while the estimated weights of the Amygdala (V_l) and the Orbitofrontal Cortex (W_l) are converging to desired targets. According to Theorem 1, estimated weights converge to desired targets asymptotically. Therefore, the designed BELBIC input u_i^{BEL} (i.e., Equation (17)) converges to distributed intelligent flocking control of networked multi-UAS asymptotically.*

4. Simulation Results

This section presents computer-based simulation results showing the performance of the proposed biologically-inspired distributed intelligent flocking control of multi-unmanned aircraft systems (Section 4.2) and multi-unmanned ground systems (Section 4.1) in an obstacle-free environment. A total of 50 unmanned aircraft and 150 unmanned ground vehicles (UGVs) were employed, with initial velocities equal to zero, and positions randomly distributed in a squared area. The following parameters are used through the simulation: $d_\alpha = 7, r = 1.2d_\alpha, d' = 0.6d_\alpha, r' = 1.2d'$. For the σ -norm, the parameter $\epsilon = 0.1$, for $\phi(z)$ the parameters $a = b = 5$, for the bump functions $\phi_\alpha(z)$ and $\phi_\beta(z)$, $h = 0.2$ and $h = 0.9$, respectively. The same network-induced delays (i.e., $\tau_{i,j} = \tau = 0.3, \forall i$) are considered for all unmanned aircrafts and unmanned ground vehicles. All simulations are carried out on a platform with following specifications: Windows Server 2012 R2 standard, Processor: Intel(R) Xeon(R) CPU E5-2680 0 @ 2.70 GHz (4 processors), RAM: 8.00 GB.

4.1. Flocking of UGVs in an Obstacle-Free Environment

Figure 3 shows two snapshots of the simulation of the multi-unmanned ground systems in the obstacle-free environment. Figure 3 Left shows the 150 UGVs in their initial positions at $t = 0$ s while Figure 3 Right shows the UGVs at $t = 40$ s where they are flocking and have successfully formed a connected network.

For comparison purposes, two similar experiments were performed, but using the flocking algorithm introduced in [3], and Multirobot Cooperative Learning for Predator Avoidance (MCLPA) flocking algorithm introduced in [36] instead of the proposed algorithm. Figure 4 shows the velocities of all UGVs on the x - and y -axis for all methods in an obstacle-free environment under the influence of the networked-induced delay. The plot shows that, although the delay is deterministic, it is unknown and the proposed method could effectively handle the influences of the network-induced delay.

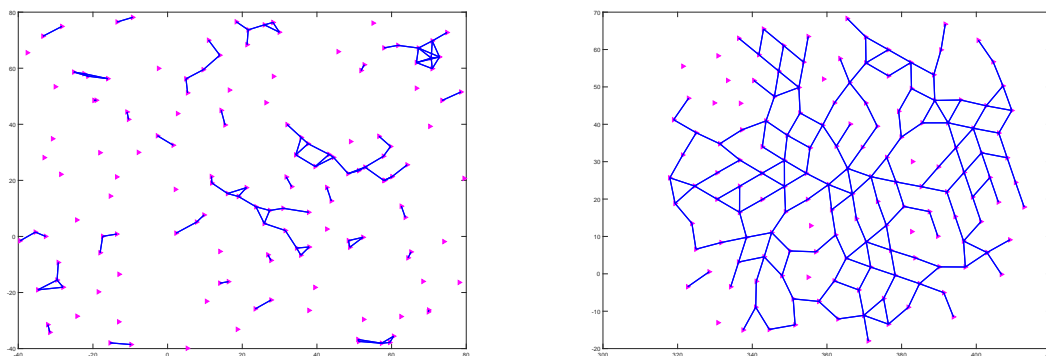


Figure 3. Simulation in an obstacle-free environment. (Left) 150 UGVs randomly distributed in a squared area at $t = 0$ s. (Right) at $t = 40$ s, the 150 UGVs are flocking and have successfully formed a connected network.

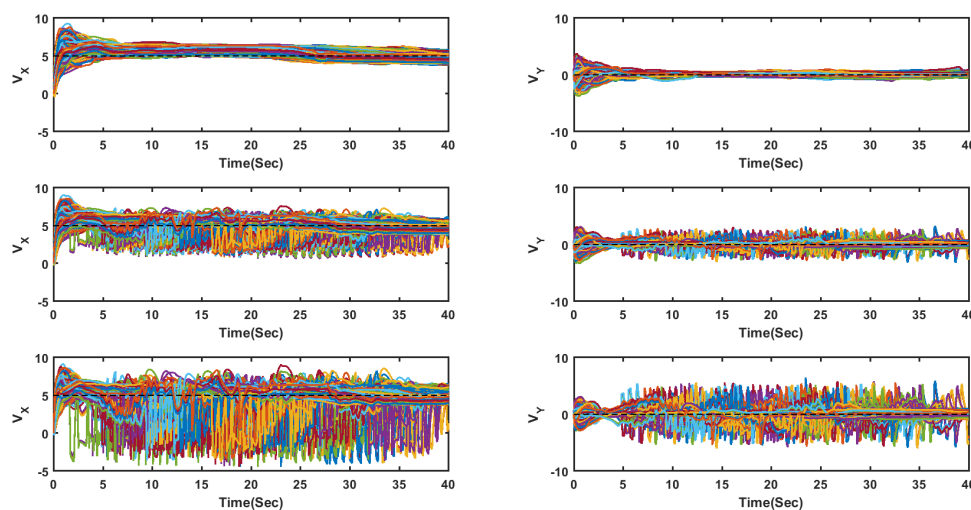


Figure 4. Velocities of all UGVs on the x - and y -axis for all methods in an obstacle-free environment under the influence of the networked-induced delay. The proposed method (top row), the MCLPA [36] (middle row), and the flocking algorithm proposed in [3] (bottom row).

Figure 5 shows the Mean Square Error (MSE) $\frac{1}{n} \sum_{i=1}^n (p_i - p_d)^2$ of the velocities of the overall group of agents, for the flocking methods in [3], the MCLPA flocking strategy in [36], and the BELBIC-based flocking, when evolving in an obstacle-free environment.

Table 1 shows the characteristics of the MSE of velocities of all flocking strategies for UGVs in the obstacle-free environment.

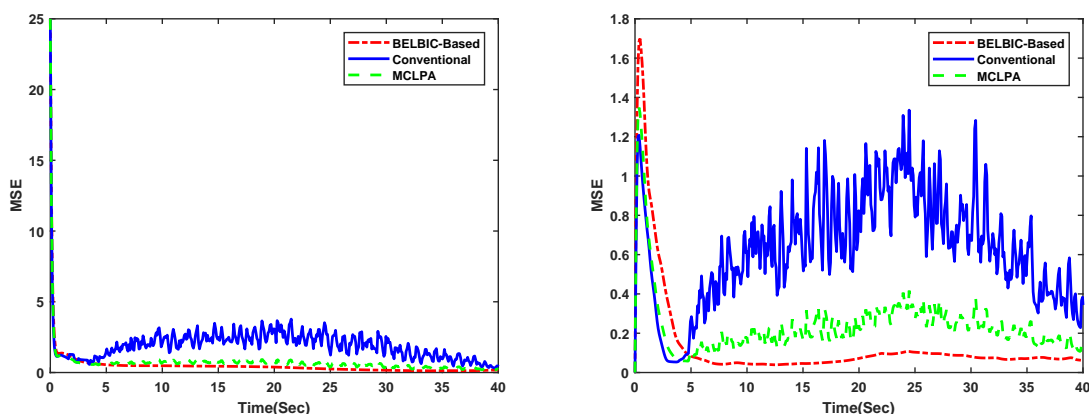


Figure 5. Mean Square value of the velocities of all UGVs on the x -axis–(Left) and y -axis–(Right) generated by the overall group of agents when flocking in an obstacle-free environment. The BELBIC-based flocking is presented in dot-dashed red, the MCLPA flocking strategy in [36] in dashed green, and the flocking in [3] in solid blue. Notice that the MSE of the BELBIC-based flocking are smaller, and therefore more appropriate to implement in real-robots.

Table 1. Characteristics of the MSE of all flocking strategies for UGVs in the obstacle-free environment.

	Flocking in [3]	MCLPA [36]	BELBIC-Based
Mean Value on the x -axis	0.802	0.641	0.602
Standard Deviation on the x -axis	6.025×10^{-5}	5.566×10^{-5}	0.814×10^{-5}
Mean Value on the y -axis	0.371	0.245	0.176
Standard Deviation on the y -axis	6.869×10^{-4}	3.068×10^{-4}	1.324×10^{-4}

4.2. Flocking of UASs in an Obstacle-Free Environment

Figure 6 shows two snapshots of the simulation of the multi-unmanned aircraft systems in the obstacle-free environment. Figure 6 Left shows the 50 UASs in their initial positions at $t = 0$ s while Figure 6 Right shows the UASs at $t = 40$ s where they are flocking and have successfully formed a connected network.

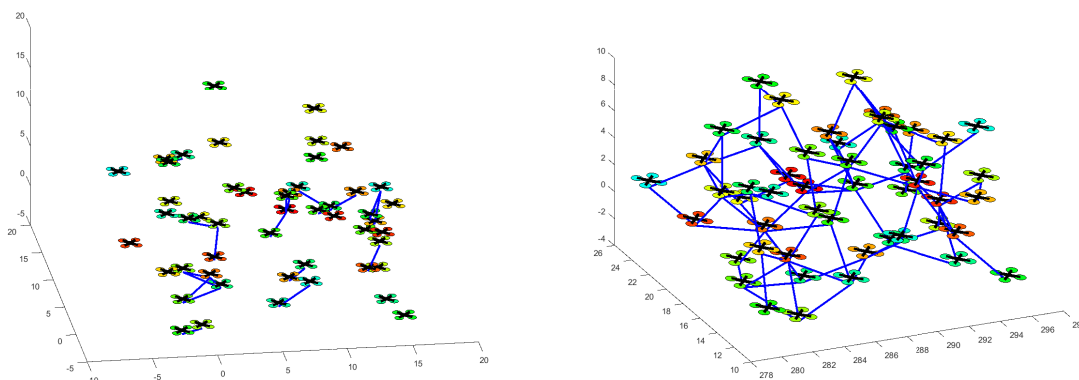


Figure 6. Simulation in an obstacle-free environment. (Left) 50 UASs randomly distributed in a squared area at $t = 0$ s; (Right) At $t = 40$ s, the 50 UASs are flocking and have successfully formed a connected network.

For comparison purposes, two similar experiments were performed, but using the flocking algorithm introduced in [3], and Multirobot Cooperative Learning for Predator Avoidance (MCLPA) flocking algorithm introduced in [36] instead of the proposed algorithm. Figure 7 shows the velocities

of all UASs on the x - and y -axis for all methods in an obstacle-free environment under the influence of the networked-induced delay. The plot shows that, although the delay is deterministic, it is unknown and the proposed method could effectively handle the influences of the network-induced delay.

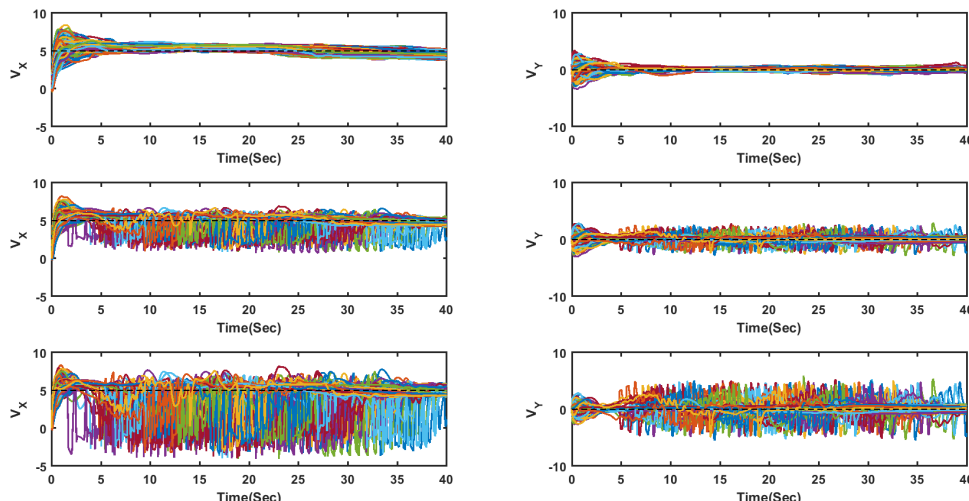


Figure 7. Velocities of all UASs on the x and y -axis for all methods in an obstacle-free environment under the influence of the networked-induced delay. The proposed method top row, the MCLPA [36] middle row, and the flocking algorithm proposed in [3] the bottom row.

Figure 8 shows the Mean Square Error $\frac{1}{n} \sum_{i=1}^n (p_i - p_d)^2$ of the velocities of the overall group of agents, for the flocking methods in [3], the MCLPA flocking strategy in [36], and the BELBIC-based flocking, when evolving in an obstacle-free environment.

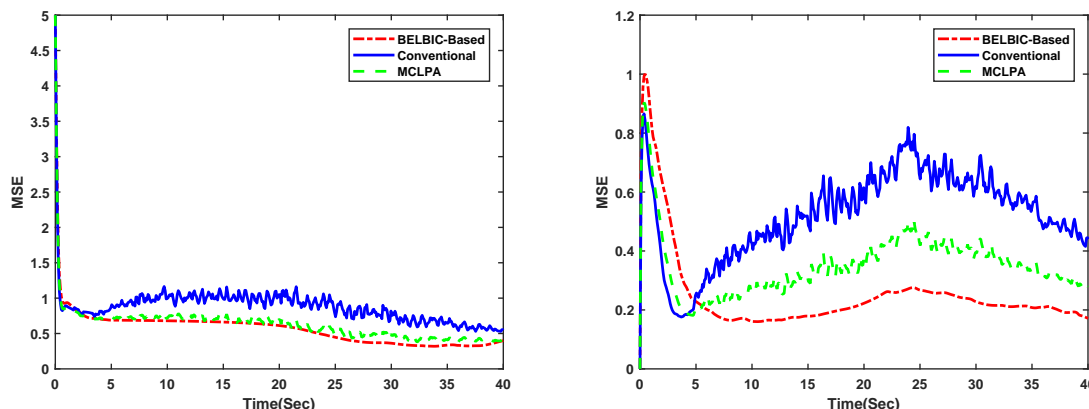


Figure 8. Mean Square value of the velocities of all UAVs on the x -axis–(Left) and y -axis–(Right) generated by the overall group of agents when flocking in an obstacle-free environment. The BELBIC-based flocking is presented in dot-dashed red, the MCLPA flocking strategy in [36] in dashed green, and the flocking in [3] in solid blue. Notice that the MSE of the BELBIC-based flocking are smaller, and therefore more appropriate to implement in real-robots.

Table 2 shows the characteristics of the MSE of velocities of all flocking strategies for UAVs in the obstacle-free environment.

Table 2. Characteristics of the MSE of all flocking strategies for UAVs in the obstacle-free environment.

	Flocking in [3]	MCLPA [36]	BELBIC-Based
Mean Value on the x -axis	0.762	0.581	0.512
Standard Deviation on the x -axis	5.726×10^{-5}	5.065×10^{-5}	0.764×10^{-5}
Mean Value on the y -axis	0.356	0.225	0.147
Standard Deviation on the y -axis	6.439×10^{-4}	2.805×10^{-4}	1.042×10^{-4}

5. Conclusions

The challenges of network-induced delay in flocking of networked multi-unmanned aircraft systems have been studied in this paper. A biologically-inspired distributed intelligent control methodology based on the emotional learning phenomenon in the mammalian limbic system has been proposed to overcome these challenges. Considering the influence of network-induced delay in real-time networked multi-unmanned aircraft systems flocking, the proposed technique demonstrated to be a promising tool for practical implementation because of its learning capability and low computational complexity. Computer-based numerical results of the implementation of the proposed methodology show the effectiveness of this algorithm for distributed intelligent flocking control of networked multi-UAS.

Future work will consider the implementation of a biologically-inspired intelligent control strategy for addressing real-world scenarios such as tracking, search and rescue, underwater explorations, etc.

Author Contributions: Conceptualization, M.J.; Methodology, M.J.; Software, M.J.; Validation, M.J. and H.X.; Formal Analysis, M.J.; Investigation, M.J.; Resources, M.J. and H.X.; Data Curation, M.J.; Writing-Original Draft Preparation, M.J.; Writing-Review & Editing, M.J. and H.X.; Visualization, M.J.; Supervision, H.X.; Project Administration, M.J. and H.X.; Funding Acquisition, H.X.

Funding: This research received no external funding.

Conflicts of Interest: The authors declare no conflict of interest. The funders had no role in the design of the study; in the collection, analyses, or interpretation of data; in the writing of the manuscript, and in the decision to publish the results.

Appendix A.

Appendix A.1. Non-Adapting Phase

Our goal is to investigate the output of the system in non-adapting phase (i.e., when the system completes its learning process) so the Equations (10) and (11) which are the updating rules of Amygdala and Orbitofrontal Cortex, respectively, should be taken into consideration. In addition, we make an assumption that the *max* function in Equation (10) could be neglected. By substituting (8) and (9) in Equation (7), the output of the model could be defined as follows:

$$\begin{aligned}
 MO &= \sum_l V_l S_l - \sum_l W_l S_l \\
 &= \sum_l (V_l - W_l) S_l,
 \end{aligned} \tag{A1}$$

$$\begin{aligned}
 \Delta V_l &= K_v S_l \left(ES - \sum_l A_l \right) \\
 &= K_v S_l \left(ES - \sum_l V_l S_l \right),
 \end{aligned} \tag{A2}$$

$$\begin{aligned}\Delta W_l &= K_w S_l (MO - ES) \\ &= K_w S_l \left(\sum_l (V_l - W_l) S_l - ES \right).\end{aligned}\quad (A3)$$

When the learning process is completed (i.e., after system completes its learning process), the variations of the weights of Amygdala (ΔV_l) and Orbitofrontal Cortex (ΔW_l) will be equal to zero (i.e., $\Delta V_l = \Delta W_l = 0$). With the assumption of $S_l \neq 0$, the following holds:

$$\begin{aligned}K_v S_l \left(ES - \sum_l V_l S_l \right) &= 0 \\ \Rightarrow \sum_l V_l S_l &= ES,\end{aligned}\quad (A4)$$

$$\begin{aligned}K_w S_l \left(\sum_l (V_l - W_l) S_l - ES \right) &= 0 \\ \Rightarrow \sum_l (V_l - W_l) S_l &= ES \\ \Rightarrow \sum_l W_l S_l &= 0.\end{aligned}\quad (A5)$$

By substituting (A4) and (A5) in Equation (A1), the model output in non-adapting phase will be as follows:

$$MO = \sum_l (V_l - W_l) S_l = \sum_l V_l S_l = ES. \quad (A6)$$

Appendix A.2. Main Proof

Considering the results obtained in Subsection A.1, the following should be achieved:

$$MO_l \rightarrow ES_l. \quad (A7)$$

Let us consider that V_l^* is the weight of Amygdala for each control input l when the system has been learned and let $\hat{E}S_l$ be the Emotional Signal for each control input l during the adaptation phase. The following hold:

$$ES_l = V_l^* S_l \text{ and } \hat{E}S_l = V_l S_l, \quad (A8)$$

$$\Delta V_l(k) = K_v S_l \max(0, ES_l - \hat{E}S_l). \quad (A9)$$

We will investigate the results of the following two cases:

- I. $ES_l - \hat{E}S_l \geq 0$,
- II. $ES_l - \hat{E}S_l < 0$.

Considering case I, the proof can be achieved as follows:

$$\begin{aligned}\Delta V_l(k) &= K_v S_l \max(0, ES_l - \hat{E}S_l) \\ &= K_v S_l (ES_l - \hat{E}S_l) \\ &= K_v S_l (V_l^* S_l - V_l S_l) \\ &= K_v S_l (V_l^* - V_l) S_l \\ &= K_v S_l \tilde{V}_l S_l \\ &= K_v \tilde{V}_l (S_l)^2,\end{aligned}\quad (A10)$$

where $\tilde{V}_l = V_l^* - V_l$,

$$\begin{aligned} V_l(k+1) &= V_l(k) + \Delta V_l(k) \\ \tilde{V}_l(k+1) &= V^* - V_l(k) - \Delta V_l(k) \\ &= \tilde{V}_l(k) - K_v \tilde{V}_l(SI_l)^2 \\ &= [1 - K_v(SI_l)^2] \tilde{V}_l(k). \end{aligned} \quad (\text{A11})$$

Considering case II, it is obvious that, when $ES_l - \hat{E}\hat{S}_l < 0$, the max function in Equation (A9) will force the adaptation in the Amygdala to stop and the following hold:

$$\begin{aligned} \Delta V_l(k) &= 0, \\ V_l(k+1) &= V_l(k), \\ \tilde{V}_l(k+1) &= \tilde{V}_l(k). \end{aligned} \quad (\text{A12})$$

The proof can be achieved as follows:

$$\begin{aligned} \Delta W_l(k) &= K_w SI_l (MO_l - ES_l) \\ &= K_w SI_l (V_l SI_l - W_l SI_l - V_l^* SI_l) \\ &= K_w SI_l (- (V_l^* - V_l) SI_l - W_l SI_l) \\ &= K_w SI_l ((-\tilde{V}_l - W_l) SI_l) \\ &= -K_w \tilde{W}_l (SI_l)^2, \end{aligned} \quad (\text{A13})$$

where $\tilde{V}_l = V_l^* - V_l$ and $\tilde{W}_l = \tilde{V}_l + W_l$.

$$\begin{aligned} W_l(k+1) &= W_l(k) + \Delta W_l(k) \\ \tilde{W}_l(k+1) &= \tilde{V}_l(k+1) + W_l(k+1) \\ &= \tilde{V}_l(k) + W_l(k) + \Delta W_l(k) \\ &= \tilde{W}_l(k) - K_w \tilde{W}_l (SI_l)^2 \\ &= [1 - K_w (SI_l)^2] \tilde{W}_l(k). \end{aligned} \quad (\text{A14})$$

Appendix B.

Let's consider that u_s is a stable controller for the following system:

$$\dot{x} = f(x) + g(x)u_s. \quad (\text{A15})$$

There is a Lyapunov function $L_s(x)$ that guarantees the stability of the whole system:

$$L_s(x) = \frac{1}{2} x^T x.$$

Taking the first derivative, we have:

$$\begin{aligned} \dot{L}_s(x) &= x^T \dot{x} \\ &= x^T [f(x) + g(x)u_s] \\ &\leq -lx^T x, \quad l > 0. \end{aligned} \quad (\text{A16})$$

To provide the stability analysis of the actual system, let's consider that the u_a is an actual controller for the following system:

$$\dot{x} = f(x) + g(x)u_a, \quad (\text{A17})$$

where u_a is as follows:

$$u_a = u_s + \tilde{u} \quad (\text{A18})$$

and \tilde{u} is the controller, which is given by the BELBIC model output MO . Considering the Lyapunov function $L_{MO}(x)$, the following is obtained:

$$L_{MO}(x) = A(\widetilde{MO})^2.$$

Taking the first derivative, we have:

$$\begin{aligned} \dot{L}_{MO}(x) &= A(\widetilde{MO})(\dot{\widetilde{MO}}) \\ &\leq -A(\widetilde{MO})^2 \\ &\leq -A(\tilde{u})^2. \end{aligned} \quad (\text{A19})$$

Considering the Lyapunov function $L_a(x)$, the stability proof of overall system is as follows:

$$L_a(x) = \frac{1}{2}x^T x.$$

Taking the first derivative, we have:

$$\begin{aligned} \dot{L}_a(x) &= x^T \dot{x} \\ &= x^T [f(x) + g(x)u_a] \\ &= x^T [f(x) + g(x)(u_s + \tilde{u})] \\ &= x^T [f(x) + g(x)u_s + g(x)\tilde{u}] \\ &= x^T [f(x) + g(x)u_s] + x^T g(x)\tilde{u} \\ &\leq -lx^T x + x^T g(x)\tilde{u} \\ &\leq -lx^T x + \frac{l}{2}x^T x + \frac{2}{l}(g(x)\tilde{u})^2 \\ &\leq -\frac{l}{2}x^T x + \frac{2}{l}(g(x)\tilde{u})^2 \\ &\leq -\frac{l}{2}x^T x - A(\tilde{u})^2. \end{aligned} \quad (\text{A20})$$

References

1. Reynolds, C.W. Flocks, herds and schools: A distributed behavioral model. *ACM SIGGRAPH Comput. Graph.* **1987**, *21*, 25–34. [[CrossRef](#)]
2. Olfati-Saber, R.; Murray, R.M. Consensus problems in networks of agents with switching topology and time-delays. *IEEE Trans. Autom. Control* **2004**, *49*, 1520–1533. [[CrossRef](#)]
3. Olfati-Saber, R. Flocking for multi-agent dynamic systems: Algorithms and theory. *IEEE Trans. Autom. Control* **2006**, *51*, 401–420. [[CrossRef](#)]
4. Liu, B.; Yu, H. Flocking in multi-agent systems with a bounded control input. In Proceedings of the 2009 IWCFTA'09. International Workshop on IEEE Chaos-Fractals Theories and Applications, Los Alamitos, CA, USA, 6–8 November 2009; pp. 130–134.

5. Jafari, M. On the Cooperative Control and Obstacle Avoidance of Multi-Vehicle Systems. Master's Thesis, University of Nevada, Reno, NV, USA, 2015.
6. Xu, H.; Carrillo, L.R.G. Distributed near optimal flocking control for multiple Unmanned Aircraft Systems. In Proceedings of the IEEE 2015 International Conference on Unmanned Aircraft Systems (ICUAS), Denver, CO, USA, 9–12 June 2015; pp. 879–885.
7. Jafari, M.; Sengupta, S.; La, H.M. Adaptive flocking control of multiple unmanned ground vehicles by using a uav. In Proceedings of the International Symposium on Visual Computing, Las Vegas, NV, USA, 14–16 December 2015; pp. 628–637.
8. O'Loan, O.; Evans, M. Alternating steady state in one-dimensional flocking. *J. Phys. A Math. Gen.* **1999**, *32*, L99. [[CrossRef](#)]
9. Li, S.; Liu, X.; Tang, W.; Zhang, J. Flocking of Multi-Agents Following a Leader with Adaptive Protocol in a Noisy Environment. *Asian J. Control* **2014**, *16*, 1771–1778. [[CrossRef](#)]
10. Zhang, Q.; Li, P.; Yang, Z.; Chen, Z. Adaptive flocking of non-linear multi-agents systems with uncertain parameters. *IET Control Theory Appl.* **2014**, *9*, 351–357. [[CrossRef](#)]
11. Dong, Y.; Huang, J. Flocking with connectivity preservation of multiple double integrator systems subject to external disturbances by a distributed control law. *Automatica* **2015**, *55*, 197–203. [[CrossRef](#)]
12. Jafari, M.; Xu, H.; Carrillo, L.R.G. Brain Emotional Learning-Based Intelligent Controller for flocking of Multi-Agent Systems. In Proceedings of the 2017 IEEE American Control Conference (ACC), Seattle, WA, USA, 24–26 May 2017; pp. 1996–2001.
13. Chopra, N.; Spong, M.W. Output synchronization of nonlinear systems with time delay in communication. In Proceedings of the 2006 45th IEEE Conference on IEEE, Decision and Control, Sydney, Australia, 13–15 December 2006; pp. 4986–4992.
14. Nourmohammadi, A.; Jafari, M.; Zander, T.O. A Survey on Unmanned Aerial Vehicle Remote Control Using Brain–Computer Interface. *IEEE Trans. Hum. Mach. Syst.* **2018**, *48*, 337–348. [[CrossRef](#)]
15. Wan, Z. Flocking for Multi-Agent Dynamical Systems. Master's Thesis, University of Waterloo, Waterloo, ON, Canada, 2012.
16. Yang, Z.; Zhang, Q.; Jiang, Z.; Chen, Z. Flocking of multi-agents with time delay. *Int. J. Syst. Sci.* **2012**, *43*, 2125–2134. [[CrossRef](#)]
17. Liu, Y.; Ho, D.W.; Wang, Z. A new framework for consensus for discrete-time directed networks of multi-agents with distributed delays. *Int. J. Control* **2012**, *85*, 1755–1765. [[CrossRef](#)]
18. Kar, S.; Moura, J.M. Distributed consensus algorithms in sensor networks with imperfect communication: Link failures and channel noise. *IEEE Trans. Signal Process.* **2009**, *57*, 355–369. [[CrossRef](#)]
19. Mehrabian, A.R.; Khorasani, K. Distributed formation recovery control of heterogeneous multiagent euler-lagrange systems subject to network switching and diagnostic imperfections. *IEEE Trans. Control Syst. Technol.* **2016**, *24*, 2158–2166. [[CrossRef](#)]
20. Zhang, Q.; Li, P.; Yang, Z.; Chen, Z. Distance constrained based adaptive flocking control for multiagent networks with time delay. *Math. Probl. Eng.* **2015**, 2015. [[CrossRef](#)]
21. Cao, Y.; Oguchi, T. Coordinated Control of Mobile Robots with Delay Compensation Based on Synchronization. In *Sensing and Control for Autonomous Vehicles*; Springer: Berlin, Germany, 2017; pp. 495–514.
22. Dashti, Z.A.S.; Gholami, M.; Jafari, M.; Shoorehdeli, M.A.; Teshnehlab, M. Speed control of a Digital Servo System using parallel distributed compensation controller and Neural Adaptive controller. In Proceedings of the 2013 13th Iranian Conference on IEEE, Fuzzy Systems (IFSC), Qazvin, Iran, 27–29 August 2013; pp. 1–6.
23. Jafari, M.; Xu, H.; Garcia Carrillo, L.R. A neurobiologically-inspired intelligent trajectory tracking control for unmanned aircraft systems with uncertain system dynamics and disturbance. *Trans. Inst. Meas. Control* **2018**. [[CrossRef](#)]
24. Jafari, M.; Sarfi, V.; Ghasemkhani, A.; Livani, H.; Yang, L.; Xu, H.; Koosha, R. Adaptive neural network based intelligent secondary control for microgrids. In Proceedings of the 2018 IEEE Texas Power and Energy Conference (TPEC), College Station, TX, USA, 8–9 February 2018; pp. 1–6.
25. Moren, J.; Balkenius, C. A computational model of emotional learning in the amygdala. *Anim. Anim.* **2000**, *6*, 115–124.
26. Lucas, C.; Shahmirzadi, D.; Sheikholeslami, N. Introducing BELBIC: brain emotional learning based intelligent controller. *Intell. Autom. Soft Comput.* **2004**, *10*, 11–21. [[CrossRef](#)]

27. Kim, J.W.; Oh, C.Y.; Chung, J.W.; Kim, K.H. Brain emotional limbic-based intelligent controller design for control of a haptic device. *Int. J. Autom. Control* **2017**, *11*, 358–371. [[CrossRef](#)]
28. Rizzi, C.; Johnson, C.G.; Fabris, F.; Vargas, P.A. A situation-aware fear learning (SAFEL) model for robots. *Neurocomputing* **2017**, *221*, 32–47. [[CrossRef](#)]
29. Jafari, M.; Xu, H. A Biologically-Inspired Distributed Intelligent Flocking Control for Networked Multi-UAS with Uncertain Network Imperfections. In Proceedings of the 2018 International Conference on Unmanned Aircraft Systems (ICUAS), Dallas, TX, USA, 12–15 June 2018; pp. 12–21.
30. Jafari, M.; Xu, H. Intelligent Control for Unmanned Aerial Systems with System Uncertainties and Disturbances Using Artificial Neural Network. *Drones* **2018**, *2*, 30. [[CrossRef](#)]
31. Jafari, M.; Shahri, A.M.; Shouraki, S.B. Attitude control of a quadrotor using brain emotional learning based intelligent controller. In Proceedings of the 2013 13th Iranian Conference on IEEE, Fuzzy Systems (IFSC), Qazvin, Iran, 27–29 August 2013; pp. 1–5.
32. Jafari, M.; Shahri, A.M.; Elyas, S.H. Optimal Tuning of Brain Emotional Learning Based Intelligent Controller Using Clonal Selection Algorithm. In Proceedings of the 2013 3th International eConference on IEEE, Computer and Knowledge Engineering (ICCKE), Mashhad, Iran, 31 October–1 November 2013; pp. 30–34.
33. Lin, C.M.; Chung, C.C. Fuzzy Brain Emotional Learning Control System Design for Nonlinear Systems. *Int. J. Fuzzy Syst.* **2015**, *17*, 117–128. [[CrossRef](#)]
34. Mei, Y.; Tan, G.; Liu, Z. An improved brain-inspired emotional learning algorithm for fast classification. *Algorithms* **2017**, *10*, 70. [[CrossRef](#)]
35. El-Garhy, M.A.A.A.; Mubarak, R.; El-Bably, M. Improving maximum power point tracking of partially shaded photovoltaic system by using IPSO-BELBIC. *J. Instrum.* **2017**, *12*, P08012. [[CrossRef](#)]
36. La, H.M.; Lim, R.; Sheng, W. Multirobot cooperative learning for predator avoidance. *IEEE Trans. Control Syst. Technol.* **2015**, *23*, 52–63. [[CrossRef](#)]



© 2018 by the authors. Licensee MDPI, Basel, Switzerland. This article is an open access article distributed under the terms and conditions of the Creative Commons Attribution (CC BY) license (<http://creativecommons.org/licenses/by/4.0/>).